Published in final edited form as:

Colloids Surf B Biointerfaces. 2021 October ; 206: 111952. doi:10.1016/j.colsurfb.2021.111952.

Rheumatoid arthritis treatment using hydroxychloroquine and methotrexate co-loaded nanomicelles: *In vivo* results

Tais Monteiro Magne[a], **Edward Helal-Neto**[a], **Luana Barbosa Correa**[a,g,h], **Luciana Magalhães Rebelo Alencar**[b], **Sara Gemini Piperni**[c], **Surtaj H. Iram**[d], **Prapanna Bhattarai**[e], **Lin Zhu**[e], **Eduardo Ricci-Junior**[f], **Maria das Graças Muller de Oliveira Henriques**[g,h], **Elaine Cruz Rosas**[g,h], **Ralph Santos-Oliveira**[a,i,*]

[a]Brazilian Nuclear Energy Commission, Nuclear Engineering Institute, Laboratory of Nanoradiopharmaceuticals and Synthesis of Novel Radiopharmaceuticals, Rio de Janeiro, Brazil

[b]Federal University of Maranhão, Department of Physics, Maranhão, Brazil

[c]Unigranrio, Laboratory of Multidisciplinary Studies, Rio de Janeiro, Brazil

[d]Department of Chemistry & Biochemistry, College of Natural Sciences, South Dakota State University, Brookings, 57007, SD, USA

[e]Department of Pharmaceutical Sciences, Irma Lerma Rangel College of Pharmacy, Texas A&M University, TX, USA

[f]Laboratory of Nanomedicine, Federal University of Rio de Janeiro, Rio de Janeiro, Brazil

[g]National Institute for Science and Technology on Innovation on Diseases of Neglected Populations (INCT/IDPN), Oswaldo Cruz Foundation, Rio de Janeiro, Brazil

[h]Laboratory of Applied Pharmacology, Farmanguinhos, Oswaldo Cruz Foundation, Rio de Janeiro, RJ, Brazil

[i]Zona Oeste State University, Laboratory of Radiopharmacy and Nanoradiopharmaceuticals, Rio de Janeiro, Brazil

Abstract

Rheumatoid arthritis (RA) is the most common inflammatory rheumatic disease, affecting almost 1% of the world population. It is a long-lasting autoimmune disease, which mainly affects the joints causing inflammation and swelling of the synovial joint. RA has a significant impact on the

[*]Corresponding author at: Brazilian Nuclear Energy Commission, Nuclear Engineering Institute, Ilha do Fundão, Rua Helio de Almeida, 75, Rio de Janeiro, RJ, Brazil. roliveira@ien.gov.br (R. Santos-Oliveira).

CRediT authorship contribution statement

Tais Monteiro Magne: Conceptualization, Methodology, formal analysis. **Edward Helal-Neto:** methodology, validation, formal analysis. **Luana Barbosa Correa:** formal analysis, validation. **Luciana Magalhães Rebelo Alencar:** formal analysis, investigation. **Sara Gemini Piperni:** Methodology, formal analysis, writing and review. **Surtaj H Iram:** Methodology, formal analysis, writing and review, data curation. **Prapanna Bhattarai:** methodology, validation, formal analysis. **Lin Zhu:** Methodology formal analysis, investigation, supervision, project administration, funding acquisition and write. **Eduardo Ricci-Junior:** Methodology, validation. **Maria Das Graças Muller de Oliveira Henriques:** methodology, validation, formal analysis. **Elaine Cruz Rosas:** investigation, resources, validation and conceptualization. **Ralph Santos-Oliveira:** Conceptualization, Methodology formal analysis, investigation, supervision, project administration, funding acquisition, write and review.

Declaration of Competing Interest

The authors report no declarations of interest.

ability to perform daily activities including simple work and household chores. Nonetheless, due to the long periods of pain and the continuous use of anti-inflammatory drugs, RA can debilitate the quality of life and increases mortality. Current therapeutic approaches to treat RA aim to achieve prolonged activity and early and persistent remission of the disease, with the gradual adoption of different drugs available. In this study, we developed a novel hydroxychloroquine and methotrexate co-loaded Pluronic® F-127 nanomicelle and evaluated its therapeutic effects against RA. Our results showed that drug-loaded nanomicelles were capable of modulating the inflammatory process of RA and reducing osteoclastogenesis, edema, and cell migration to the joint. Overall, compared to the free drugs, the drug-loaded nanomicelles showed a 2-fold higher therapeutic effect.

Keywords

Nanotherapy; Rheumatoid arthritis treatment; Methotrexate; Hydroxychloroquine

1. Introduction

Rheumatoid arthritis (RA) is a systemic autoimmune disease of unknown etiology, characterized by a complex interaction between immune mediators (cytokines and effector cells) responsible for joint damage that begins in the synovial membrane [1]. The pathophysiology of RA is complex and involves the proliferation of synovial cells and fibrosis, formation of *pannus*, with erosion of cartilage and bone [2]. In the long term, the pathophysiological process of RA results in joint degradation associated with pain, stiffness, loss of function and systemic comorbidities, reducing life expectancy and quality of life [3,4].

Despite advances in recent decades regarding the pathophysiology of RA and the development of new target therapies, there is still a considerable need to develop more effective therapies since complete remission is not maintained without continuous treatment. Current therapies for RA are limited by low drug bioavailability, high drug clearance, and dose-limiting adverse effects [5]. A promising strategy is to increase the effectiveness of existing RA drugs through drug delivery systems, such as nanoparticles [1,6–9].

Nanomicelles are one of the most widely used nanoparticles to improve the blood circulation time, bioavailability, and specificity of various therapeutic agents. Therapeutic agents (properly loaded into the nanocarrier) can be selectively accumulated in the inflamed sites through passive or active targeting after systemic administration [5]. In this way, the damage to other organs is remarkably reduced. In addition, the nanocarriers can protect the encapsulated therapeutic agents against biodegradation and provide the sustained drug release, leading to the increased drug efficacy [1,5,10,11].

The College of Rheumatology and the European League Against Rheumatism (ACR / EULAR) recommend methotrexate (MTX) at the beginning of RA as (part of) the first treatment due to its favorable balance in efficacy, safety profile and costs [12,13]. When MTX is used as a single agent, the benefits are quickly realized, but tend to stabilize after about 6 months of treatment [14]. The literature shows that the combined use of

MTX with other disease-modifying antirheumatic drugs (DMARDs) makes therapy more effective. Among the combined therapies for the treatment of RA, the use of MTX with the antimalarial drug Hydroxychloroquine (MTX + HCQ) has been showing good results in clinic. However, studies on the effectiveness of the combined use of these drugs and the mechanisms of action were not investigated.

In this study, we prepared and characterized Pluronic® F-127 nanomicelles co-loaded with HCQ and MTX (127-Pluronic–HCQ-MTX) and evaluated *in vitro* and *in vivo* efficacy against RA. We demonstrated that 127-Pluronic–HCQ-MTX nanomicelles loaded with 50 % of the recommended doses used in the clinic significantly reduced osteoclastogenesis, edema, and cell migration to the joint in the antigen-induced arthritis animal model. In addition, the 127-Pluronic–HCQ-MTX nanomicelles could improve the accumulation of HCQ and MTX in the cells by modulating MRP1.

2. Methodology

2.1. Reagents

Phosphate buffered saline (PBS), PBS/EDTA (ethylenediamine tetraacetic acid) (10 mM) freshly prepared solution, bovine serum albumin (BSA), methylated bovine serum albumin (mBSA), Freund's complete adjuvant, Histopaque reagent, Pluronic F127, TRAcP staining kit, DMEM high glucose, Bovine fetal serum, M-CSF, RANK-L, Doxorubicin, Poly-D-lysine, Glucose, HEPES, Calcium and Magnesium were purchased from Sigma Aldrich (St. Louis, MO, USA). MayGrünwald and Giemsa dyes were purchased from Merck (Germany). 3% sodium pentabarbital (Hypnol®) was purchased from Syntec (Brazil). Tevametho (injectable methotrexate 25 mg/mL) was purchased from Teva Farm-acêutica Ltda (Brazil) and Hydroxychloroquine was purchased from Sigma Aldrich.

2.2. Preparation of the nanomicelles

A concentration of 0,3 mg/mL of hydroxychloroquine and 0,6 mg/mL of methotrexate were added in the micellar dispersion of Pluronic F127. The system was gently stirred using a magnetic bar (Magnetic Stirrer, IKA, C-MAG HS-7) and then processed for 5 min using an ultrasonic processor (UP100H, Hielscher, Power: 100 %, Cycle: 1) under ice bath at 10 °C.

2.3. Particle size and zeta potential

The particle size, size distribution, and polydispersity index (PDI) of nanosystem were determined by dynamic light scattering (DLS) using the equipment Zetasizer Nano ZS (Malvern Instruments, UK). Measurements were performed in triplicate at 25 °C and the laser incidence angle in relation to the sample was 173° using a 12 mm^2 quartz cuvette. The mean ± standard deviation (SD) was assessed. The zeta potential from each nanosystem has been performed using a Litesizer 500 (Anton Paar, Germany). Measurements were performed at 20 °C and the laser incidence angle in relation to sample was 15°, using an Omega shaped cuvette. All data is a mean of 1000 runs.

2.4. Atomic force microscopy (AFM)

The AFM analysis has been performed using a Multimode 8 microscope (Bruker, Santa Barbara, CA). Two main analyses have been conducted in the sample (127-Pluronic–HCQ-MTX-nanomicelles): First, the morphology and topography of the nanomicelles were analyzed, comparing the sizes observed in the AFM images with the DLS results. In addition, nanomechanics maps of the micelles were obtained by acquiring approximately 65,000 force curves over each scanning area. For these measurements, Scanasyst Air probes were used, with a nominal spring constant of 0.4 N/m, however, the actual spring constant of each probe was calibrated by the thermal noise method. A drop of the nanomicelles solution was deposited in freshly cleaved mica to form the nanomicelles film. The scanning mode used was Peak Force Tapping Quantitative Nanomechanics (QNM), with a resolution of 256 × 256 lines per scan and scan frequency of 0.5 Hz.

2.5. In vitro drug release

The drug release profiles of the 127-Pluronic–HCQ-MTX-nanomicelles were studied by a well-established dialysis method [15,16]. Briefly, 400 μL of the nanomicelles were placed in the dialysis bag (MWCO 12000–14000 Da). The dialysis bag was suspended and stirred in 30 mL of PBS containing 0.1 % Tween 80 at 37 °C to simulate the “sink condition”. 300 μL of the outside medium were collected at the scheduled time points over 24 h. The released HCQ and MTX were quantified by the microplate reader at the wavelengths of 340 nm and 310 nm, respectively.

2.6. Osteoclastogenesis assay

Cell isolation: monocytes were isolated from peripheric blood of volunteers through density gradient centrifugation. Briefly, blood is stratified 1:1 on Histopaque reagent (Sigma Aldrich) and centrifuged during 30 min at 400 RCF with no break and acceleration. After, cells were washed twice and seeded with density of $2{,}4 \times 10^6$ cells/cm^2 3 h in controlled humified atmosphere at 37 °C 5% CO_2. After 3 h medium culture was replaced with DMEM high glucose supplemented with 10 % bovine fetal serum and 20 ng/mL M-CSF during 3 days to induce monocyte proliferation.

127-Pluronic–HCQ-MTX-nanomicelles exposition: After 3 days cells were treated with in DMEM high glucose supplemented with 10 % bovine fetal serum and 20 ng/mL M-CSF and 30 ng/mL RANK-L with or without nanomicelles with a concentration of 20 μg/mL HCQ - 0.74 ng/mL MTX or 70 μg/mL HCQ – 2,6 ng/mL MTX nanomicelles respectively. Treatment was replaced each 3 days during 14 days. Following cells were fixed and stained with TRAcP kit staining (Sigma Aldrich) and numbers of osteoclasts (multinucleated TRAcP positive cells) were quantified.

3. Rheumatoid arthritis model

3.1. Animals

Male C57BL/6 mice (20–30 g) (n = 30) were maintained on a 12 h-light/dark cycle with controlled temperature with food and water *ad libitum*. The animal study was conducted in accordance with the ethical guidelines of the International Association for the Study of Pain

and approved by Institutional Animal Care and Use Internal Review Board (license number CEUA LW-43/14).

3.2. Body weight assessment

The body weight of all animals in all groups of this study were evaluated and assessed. Thus, the animals were weighted in the begging and end of the treatment.

3.3. Induction of antigen arthritis

C57BL/6 mice were immunized by subcutaneous injection (sc) on day 0 using 500 μg of methylated bovine serum albumin (mBSA) in 0.2 mL of an emulsion containing: 0.1 mL of saline and 0.1 mL of Freund's full adjuvant. The mice were boosted with the same solution on day 07. Sham mice (fake immunized) received similar injections on day 0 and day 07, but without the antigen (mBSA). On the 21 day after the initial injection, arthritis was induced in the immunized animals by intra-articular (i.a.) injection of mBSA (30 μg/cavity; 25 μL). The sham mice received saline. From that period, the animals were treated daily, through intraperitoneal injections (100 μL/animal), for 7 days, and on the 25 day a reinjection was performed using antigen (30 μg/cavity). On day 28 mice were euthanized using excess of anesthetic (sodium pentobarbital 3% - Hypnol) for further analyzes.

3.4. Groups

The treatment was evaluated in 7 experimental groups, composed of 5 animals (mice C57Bl/6) in each group. The groups were divided into: i) false immunized: sham; ii) control group: saline; iii) immunized: mBSA; iv) vehicle group: 127-Pluronic; v) standard treatment group: Hydroxychloroquine (HCQ) plus Methotrexate (MTX) (2 mg / Kg and 1 mg / Kg, respectively); vi) intervention group 1: 127-Pluronic–HCQ-MTX nanomicelles (2 mg / K and 1 mg / Kg, respectively); vii) intervention group 2: 127-Pluronic–HCQ-MTX nanomicelles (1 mg / K and 0.5 mg / Kg, respectively).

3.5. Treatment

The standard treatment of HCQ plus MTX (2 mg/kg and 1 mg/kg, respectively) was administered intraperitoneally (i.p., 100 μL/animal). The animals in intervention group 1 were administered intraperitoneally (100 μL/animal) with nanomicelles loaded with HCQ and MTX at the same dose as the standard treatment (127-Pluronic–HCQ-MTX nanomicelles, 2 mg/kg and 1 mg/kg, respectively), while the animals in intervention group 2 were administered intraperitoneally (100 μL/animal) with HCQ and MTX-loaded nanomicelles in the half dose of the standard treatment (127-Pluronic–HCQ-MTX nanomicelles, 1 mg/kg and 0.5 mg/kg, respectively).

The animals in the control group (saline) and in the immunized group (mBSA) were administered intraperitoneally with 100 μL of sterile saline. The animals in the vehicle group were intraperitoneally administered with 100 μL of Pluronic F127 10 % solubilized in sterile saline (Table 1).

3.6. Parameters

All groups were euthanized using excess of anesthetic (sodium pentobarbital 3% Mitutoyo Corporation, Kanagawa, Japan). Knee joint thickness were evaluated and expressed in millimeters (mm). The knee synovial cavities were washed out using 300 μL of PBS/EDTA (10 mM) and leukocyte counts were performed (Coulter Z2, Beckman Coulter Inc., Brea, CA, USA). Finally, using optical microscopy, smears of cytospin (Cytospin 3, Shandon Inc., Pittsburgh, PA, USA) from cells previously stained by the May-Grunwald-Giemsa method were differentially counted and reported as numbers of cells per cavity ($\times 10^5$).

3.7. MRP1 efflux transporter protein activity

Efflux transport activity of MRP1 was measured using doxorubicin accumulation assay. This assay was performed using confocal microscopy. Sterilized cover glasses were placed in 6-well plate and covered with 0.1 mg/mL of poly-D-lysine for 10 min prior to washing with phosphate buffered saline (PBS). HEK293 T cells were plated on poly-D-lysine-coated cover glass at a density of 5×10^5 cells/well in 2 mL culture medium. Cells were transiently transfected with 2 μg of an MRP1-GFP expression vector after 24 h using 4 μg of jet PRIME Transfection Reagent with 200 μL of Transfection buffer (Polyplus-transfection SA, Illkirch, France). After 48 h, cells were pre-treated with 0.1 %, w/v 0.25 % w/v, 0.5 % w/v and 1% w/vof 127-Pluronic–HCQ-MTX nanomicelles for 30 min, before incubation with doxorubicin (10 μM) for 1 h. Cells were maintained in buffer (4.5 % glucose, 10 mM HEPES, PBS containing Ca^{2+} and Mg^{2+}) as intracellular fluorescence was visualized using an iMIC digital microscope (TILL Photonics GmbH, Gräfelfing, Germany) equipped with a 1.35 numerical aperture 60x oil-immersion objective. Excitation was done at 488 nm for GFP and doxorubicin, with emission bands of 475/42 and 605/64 nm, respectively. Images were processed using ImageJ (NIH, Bethesda, MD).

3.8. Flow cytometry-based Calcein-AM accumulation assay

The effect of nanomicelle (127-Pluroni–HCQ-MTX nanomicelles) on MRP1 mediated efflux of calcein-AM was ascertained using flow cytometry. HEK 293 overexpressing MRP1 cells were prepared in serum-free medium at a density of 7×10^5 cells/mL and treated with various concentrations (0.1 %, 0.25 %, 0.5 % and 1%) of 127-Pluronic–HCQ-MTX nanomicelle for 10 min at 37 °C. Cells were then treated with calcein-AM (0.25μM) for 30 min. Final DMSO concentration was maintained at less than 1% (v/v). MRP1 mediated efflux activity was stopped using ice-cold PBS buffer (3 mL). Cells were collected, washed twice with PBS, and re-suspended in a cold PBS buffer containing 1% paraformaldehyde. Intracellular calcein-AM fluorescence was detected using BD Accuri C6 flow cytometer (BD Biosciences, San Jose, CA) with excitation and emission at 480 nm and 533/30 nm respectively. Fluorescent intensity was determined as a mean of 10,000 events. Treatments were done in triplicates and repeated in two independent experiments.

3.9. Statistical analysis

The results were expressed as the mean ± standard error of the mean (EPM) and analyzed statistically through the analysis of variance test (ANOVA), followed by the Newman-Keuls-Student or Tukey test for comparison between more than two groups. Student's "t" test was

used to compare two experimental groups. All tests were performed using GraphPad Prism 5.00 (GraphPad Software, La Jolla, California, USA). P values less than or equal (≤) to 0.05 were considered significant (*; +).

4. Results

4.1. Average size determination by dynamic light scattering and zeta potential

The hydrodynamic diameter of the nanosystem was 48,323 nm (SD 4842 nm). The PDI value was 0256 (SD 196) and zeta potential was 059 mV (SD 008 mV). The PDI value of the nanomicelle is very near of the limit of a monodispersive behavior PDI (0,3). However, for pharmaceutical purposes we assumed the limit of 0.3 and for that reason the nanomicelle showed a monodispersive behavior. The zeta potential analysis showed a mean zeta potential of 059 mV, with a conductivity of 391 mS/cm and electrophoretic mobility of 005 μm.cm/Vs (Table 2).

4.2. Atomic force microscopy maps

The Fig. 1 shows the results of topography (peak force error - Fig. 1a and d), Young's modulus (Fig. 1b and e) and adhesion (Fig. 1c and f). Topographic images reveal micelles with diameters of 1.41 μm and 1.06 μm, respectively. The Young's modulus maps show two very distinct elastic characteristics: in the center of the micelle, a region with greater Young's modulus (lighter region), and around that region, a shell with a lower E value, indicating composite materials, in this case, the drug core and the polymeric shell (127-Pluronic). The adhesion images show the same characteristic of heterogeneous material, in this case, the core has higher adhesion force values, and the polymer has lower adhesion values. This is interesting because loaded micelles have a greater adhesion strength, improving adhesion in the drug delivery target.

4.3. In vitro drug release

The in vitro drug release profile is showed in Fig. 2.

4.4. Osteoclastogenesis assay

In this study, osteoclastogenesis assay was conducted exposing monocyte from human peripheral blood to nanomicelles formed by combination of Methotrexate and Hydroxychloroquine (127-Pluronic–HCQ-MTX nanomicelles) in two different concentrations, 20 ug/mL HCQ with 074 ng/mL MTX and 70 ug/mL HCQ with 2,6 ng/mL MTX. Four nanomicelles dilutions were tested (1:10, 1:100, 1:1000 and 1:2000) with the purpose of studying the more effective concentration to use in RA treatment. Our results showed a dose dependent decrease of osteoclastogenesis in both concentrations tested compared to control (Fig. 3 A and B).

4.5. MRP1 efflux transporter protein activity

Our results showed approximately 40–50% MRP1 inhibition, meaning the nanomicelle can improve the drug accumulation in the cell further supporting our overall findings. We tested

four different concentrations (0.1 %, 0.25 %, 0.5 % and 1%) and interestingly 0.1 % (the lowest of the tested concentrations) produced the highest MRP1 inhibition (Fig. 4).

5. Rheumatoid arthritis model

5.1. Body weight assessment

In order to make sure that the treatment under study does not change body weight, the animals were weighed at the beginning and at the end of the treatment. As seen in Fig. 5, treatments with HCQ + MTX, 127-Pluronic–HCQ-MTX nanomicelles 1 and 127-Pluronic–HCQ-MTX nanomicelles 2 did not promote weight loss (Fig. 5A).

5.2. Antigen-Induced Arthritis (AIA)

In the antigen-induced arthritis (AIA) model, mice were previously immunized and challenged with mBSA via i.a. The antigen injected i.a. binds to cartilage and activates the local immune response, causing edema and progressive synovitis. In the present study, after RA induction and intraperitoneal treatment, the measurements of the transverse diameter of the femur-tibial joint of the animals were evaluated. The results obtained demonstrate that the challenge with mBSA induced a strong joint edema in animals previously immunized and untreated (mBSA) compared to the group of false-immunized (sham). The animals treated with HCQ + MTX, 127-Pluronic–HCQ-MTX nanomicelles 1 and 127-Pluronic–HCQ-MTX nanomicelles 2 for seven days showed significant inhibition of the formation of joint edema induced by the antigen compared to the mBSA group. In addition, animals administered with a vehicle (Pluronic) did not show a significant reduction in edema compared to the mBSA group (Fig. 5B).

5.3. Analysis of the influx of cells to the joint and number of circulating leukocytes

The activation of the local immune response due to the binding of the antigen to the cartilage, promotes increased vascular permeability and cell migration. We observed that animals immunized and challenged with mBSA (mBSA group) showed a significant increase in the number of leukocytes in the synovial cavity compared to the control group (saline). The animals treated with HCQ + MTX, 127-Pluronic–HCQ-MTX nanomicelles 1 and 127-Pluronic–HCQ-MTX nanomicelles 2 showed significant inhibition of cell migration to the joint cavity. It was also observed that the administration of mBSA in false immunized animals (sham) was not able to promote a significant migration of cells to the joint cavity and that the administration of the vehicle (pluronic) was not able to significantly reduce the number of leukocytes in the synovial cavity compared to the mBSA group (Fig. 6A). However, as shown in Fig. 6B, AR induction by antigen and treatments did not change the number of total circulating leukocytes

6. Discussion

The size of 48,323 nm is the expected range. For instance, Rollet et al. [17] used folic acid-functionalized nanocapsules with a size range of 443 nm for the treatment of RA, with success. The size of micellar nanosystems can vary substantially. For instance, Zhang et al. [18] developed Pluronic F127 nanomicelles with sizes varying from 45 and 160 nm.

Additionally, Zhang et al. [19] developed nanomicelles using Pluronic F68 with a size of 94.38 ± 2.68 nm. Chen et al. [20] developed Pluronic P123 nanomicelles with size lower than 200 nm. Finally, Ahmad et al. [21] stated that nanomicelles can be formed of particles with size varying from 10 nm to 200 nm.

Also, is important to consider that Pluronic nanomicelles, developed in this study were prepared at lower temperatures. Recent advances in nanomicelle delivery systems have observed that pluronic F127 nanomicelles can increase in size according to the physical properties of the medium, such as pH and temperature [22]. Basak et al. [23] demonstrated that the hydrodynamic radii of nanomicelles increase with decreasing temperature. According to the authors, the increase in micellar sizes due to the decrease in temperature is accompanied by an increase in the hydration of the micellar core, while the increase in temperature results in more compact micelles by excluding the solvent from the micellar core due to the hydrophobic characteristics of the core.

Regarding the entrapment efficacy, we assumed a 100 % encapsulation since we have used the bulk of nanomicelle without any further treatment [24–27]. Is important to notice however, that several techniques can be used to purify as dry the solely nanomicelle as a powder ready-to-use. For example: Masoumi et al. [28]; Arbain et al. [29]; Feng et al. [30] and Jyotshna et al. [31], centrifuged the nanomicelle in order to obtain the powder. On the other hand, several studies have used the bulk of nanomicelle, considering the encapsulation as 100 %. For instance, Carvalho et al. [24], Raval et al. [25], Meng et al. [26] and Jaiswal et al. [27] assumed that nanomicelles have 100 % of encapsulation, when the nanomicelle in solution without any further step, as a bulk. Finally, is important to notice that nanomicellar dispersions are kinetically stable and homogeneous and there is a technical limitation to separate the nanomicelles from aqueous external medium or dispersing medium. Regarding the PDI, according to Danaei et al. [32] demonstrated that a dispersion with polydispersity index (PDI) value varying from 0.1 to 0.5, for pharmaceutical products, may be considered a monodisperse system. Also, according to Han and Jiang [33] a PDI value higher than 0.1 but lower than 0.3, can be defined as monodispersive. Thus, we considered a monodisperse nanosystem. The nanoparticle presented a zeta potential of 059 mV. According to Frohlich [34] the charge is essential for the nanosystem penetration. Positively charged nanosystems seems to have a facilitate traffic into the cell while negatively charged nanosystem shows a more difficult cell-trafficking. Thus, the charge seems adequate for the purposed use of the nanosystem developed.

The 127-Pluronic nanomicelles (127-Pluronic–HCQ-MTX nanomicelles) prolonged the release of both HCQ and MTX, compared to the free drugs. The results corroborated the functionality of pluronic nanomicelles as controlled release nanosystems for drug delivery [35–39]. The Pluronic–HCQ-MTX-nanomicelles showed the initial “burst drug” release, probably due to the unentrapped drugs in the micelle suspension [40].

Rheumatoid Arthritis (RA) is an autoimmune disease defined by bone and cartilage degradation, caused by a continuous inflammation of the synovium, which leads to the swelling of the joints. Depending on the gravity of this disease, it may evolve and develop cardiovascular, skeletal and pulmonary disorders [41].

Our results show a reduction in osteoclasts formation directly proportional with Methotrexate-Hydroxychloroquine nanomicelle concentration. Concentration of 20 ug/mL HCQ with 074 ng/mL MTX and 70 ug/mL HCQ with 2,6 ng/mL MTX. And its dilution of 1:10 didn't allow the formation of osteoclasts at all, while following dilution of 1:100, 1:1000 and 1:2000 showed a dose response reduction in osteoclasts number. This supposedly will prevent this cell to degrade the bone tissue, providing a delay in RA evolution.

Methotrexate is considered a first line drug used for treating this disease, being used in adults, children or elderly patients, having its dose balanced according to the age, weight and particularities of each individual [41]. It was developed by Yellapregada Subbarao for the treatment of cancer, being used since 1947 [41] at high doses for leukemia, from 15 to 30 mg. Years later, it was found that when prescribed in lower doses, from 7,5 to 10 mg, it was efficient in patients with Rheumatoid Arthritis [42]. It is usually prescribed in an early diagnosis, but according to published papers, the effects of this medication should be supervised because the optimal dose of 25 mg [43], may cause some severe side effects in some patients such as hair loss, hepatotoxicity and nausea [44]. For a dual therapy, Methotrexate is often combined with some biological agents that work as second-line drugs, such as tumor necrosis factor inhibitors.

Literatures show that Disease Modifying Anti-Rheumatic Drugs (DMARDs) are more effective than the Methotrexate when used alone, despite this medication still being largely used by many rheumatologists [45]. Hydroxychloroquine is an antimalarial drug that was accidentally found to be effective against rheumatic diseases. Despite not undergoing the conventional method of drug development, it has become a common treatment for various diseases, one of them being RA [46]. However, more recent studies have explored the combination of Methotrexate with Hydroxychloroquine (MTX + HCQ), which have proven to be more effective than a monotherapy by Methotrexate alone. There's a lack of studies being carried about the efficiency of this mix of medications and to elucidate its mechanism of action. However, a study showed that 25 mg/week MTX, plus HCQ 400 mg/day, reaching maximum dose within 4–8 weeks improved RA prognostics in human patients [47]. Our results showed how a significant lower dose *in vitro* is sufficient to inhibit osteoclastogenesis, when the two drugs are combined in nanomicelle. These results open new prospective to reduce drugs concentration with this new nanomicelle formulation, enhancing curative efficiency with lower rate adverse effects.

Interestingly, we observed that the lowest of the tested concentrations of 127-Pluronic–HCQ-MTX nanomicelles (0.1 %) was the one that promoted the greatest inhibition of protein 1 related to multiple drug resistance (MRP)-1. MRP-1 is a well-established member of the super-family of ATP Binding Cassette (ABC) transporters that function as efflux pumps responsible for the MDR (multidrug resistance) phenotype [48]. According to their broad substrate specificity, these carriers can interfere with the absorption and distribution of many therapeutic agents, influencing serum concentration and changing the efficiency of different treatments.

MTX enters cells through the reduced folate transporter (RFC) and is effluxed by several transmembrane proteins, including MRPs [49]. It is hypothesized that the overexpression of these transporters may be a cause of suboptimal response to MTX, since the clinical efficacy depends, in part, on the intracellular retention of the drug. From the results obtained, we believe that this new formulation of 127-Pluronic–HCQ-MTX nanomicelles, in addition to enabling the reduction of the treatment dose, may also favor the inhibition of drug resistance mechanisms, via inhibition of MRP-1, increasing efficiency therapy.

Considering the complexity of the pathophysiological process of RA, we investigated the effects of 127-Pluronic–HCQ-MTX nanomicelles in an *in vivo* model of antigen-induced arthritis (AIA). The experimental model consists of immunizing mice with mBSA in potent adjuvants, followed by intra-articular injection of mBSA in saline. First, we investigated the effect of 127-Pluronic–HCQ-MTX nanomicelles on the animals' body weight, since studies indicate that anti-rheumatic treatments promote unwanted weight loss [50,51]. The results obtained demonstrate that the mice with induced arthritis and treated for seven days with nanomicelles loaded with HCQ and MTX did not present a reduction in body weight in the evaluated concentrations.

Then, we evaluated the effects of 127-Pluronic–HCQ-MTX nanomicelles on the inflammatory process of induced arthritis. AIA is a well-established and reproducible model that exhibits several characteristics similar to those seen in human RA, including edema and infiltration of immune cells into the joint [52]. The regulation of factors such as vascular permeability and cell migration in the rheumatic process is extremely important, as persistent inflammation in the joint cavity leads to the formation of pannus, along with erosion of cartilage and bone [2].

We demonstrated that nanomicelles loaded with MTX + HCQ (127-Pluronic–HCQ-MTX nanomicelles) are able to reduce the inflammatory process present in induced arthritis, significantly inhibiting edema and the influx of cells to the joint. The most interesting finding is that nanomicelles loaded with 50 % of the reference dose used in the clinic promoted the same inhibitory effects. From these results, we propose that the new formulation of MTX + HCQ in nanomicelles has similar effects to therapy with free MTX + HCQ, with the possibility of significantly reducing the dose used. It is worth mentioning that the treatment with 127-Pluronic–HCQ-MTX nanomicelles did not change the number of total circulating leukocytes, suggesting that its effects are local.

In addition to local effects, uncontrolled inflammation can lead to increased immune cells in the circulation [53]. These activated immune cells determine inflammatory mediators, including chemokines and cytokines, which further induce immune cell activation and proliferation and a subsequent synthesis of more inflammatory mediators that cause various inflammatory responses in target cells and tissues. In RA, this persistent inflammatory signaling perpetuates disease progression [54].

7. Conclusion

Our data showed the potential use of 127-Pluronic nanomicelles composed of HCQ and MTX for the treatment of RA. The results corroborated the drug release profile as a dose-response behavior. Also, the results showed that lower doses of the nanosystem showed superior anti-inflammatory results than the traditional HCQ and MTX associated as current drug, corroborating the higher efficacy of the nanosystem. Finally, the data showed a higher inhibition on MPR1 substrate avoiding drug resistance mechanism and improving the use for longer time of the nanomicelle when compared with the current treatment.

Acknowledgments

The work was partially supported by the National Cancer Institute of the National Institutes of Health (R15CA213103) and Texas A&M University T3 grant (247099) to Dr. Lin Zhu. Also, the work received financial support from CNPq (301069/2018-2), FAPERJ (Rede Nano-Saude) and CAPES (PROEXT-PPGB-UERJ) to Dr Ralph Santos-Oliveira. To FAPERJ for Research Support to Luana Barbosa Correa (E-26/201.946/2020).

References

[1]. Nogueira E, Gomes AC, Preto A, Cavaco-Paulo A, Folate-targeted nanoparticles for rheumatoid arthritis therapy, Nanomed. Nanotechnol., Biol. Med 12 (2016) 1113–1126, 10.1016/j.nano.2015.12.365.

[2]. Choudhary N, Bhatt LK, Prabhavalkar KS, Experimental animal models for rheumatoid arthritis, Immunopharmacol. Immunotoxicol 40 (2018) 193–200, 10.1080/08923973.2018.1434793. [PubMed: 29433367]

[3]. Smolen JS, Aletaha D, Barton A, Burmester GR, Emery P, Firestein GS, Kavanaugh A, McInnes IB, Solomon DH, Strand V, Yamamoto K, Rheumatoid arthritis, Nat Rev Dis Prim. 4 (2018) 18001, 10.1038/nrdp.2018.1. [PubMed: 29417936]

[4]. He Y, Xin Y, Rosas EC, Alencar LMR, Santos-Oliveira R, Peng X, Yu H, Fu J, Zhang W, Engineered high-loaded mixed-monoclonal antibodies (adalimumab, rituximab and trastuzumab) polymeric nanoparticle for rheumatoid arthritis treatment: a proof of concept, J. Biomed. Nanotechnol 16 (2021) 1254–1266, 10.1166/jbn.2020.2966.

[5]. Silvagni E, Di Battista M, Bonifacio AF, Zucchi D, Governato G, Scirè CA, One year in review 2019: novelties in the treatment of rheumatoid arthritis, Clin. Exp. Rheumatol 37 (2019) 519–534 (Accessed June 9, 2021), https://pubmed.ncbi.nlm.nih.gov/28956527/. [PubMed: 31140394]

[6]. Chuang SY, Lin CH, Huang TH, Fang JY, Lipid-based nanoparticles as a potential delivery approach in the treatment of rheumatoid arthritis, Nanomaterials. 8 (2018), 10.3390/nano8010042.

[7]. Lorscheider M, Tsapis N, ur-Rehman M, Gaudin F, Stolfa I, Abreu S, Mura S, Chaminade P, Espeli M, Fattal E, Dexamethasone palmitate nanoparticles: an efficient treatment for rheumatoid arthritis, J. Control. Release 296 (2019) 179–189, 10.1016/j.jconrel.2019.01.015. [PubMed: 30659904]

[8]. Ni R, Song G, Fu X, Song R, Li L, Pu W, Gao J, Hu J, Liu Q, He F, Zhang D, Huang G, Reactive oxygen species-responsive dexamethasone-loaded nanoparticles for targeted treatment of rheumatoid arthritis via suppressing the iRhom2/TNF-α/BAFF signaling pathway, Biomaterials. 232 (2020), 10.1016/j.biomaterials.2019.119730.

[9]. Moia VM, Leal Portilho F, Almeida Pádua T, Barbosa Corrêa L, Ricci-Junior E, Cruz Rosas E, Magalhaes Rebelo Alencar L, Savio Mendes Sinfronio F, Sampson A, Hussain Iram S, Alexis F, de OliveiraHenriques MD, Santos-Oliveira R, Lycopene used as anti-inflammatory nanodrug for the treatment of rheumathoid arthritis: animal assay, pharmacokinetics, ABC transporter and tissue deposition, Colloids Surf. B Biointerfaces 188 (2020), 10.1016/j.colsurfb.2020.110814.

[10]. dos Santos Matos AP, Lopes DCDXP, Peixoto MLH, da Silva Cardoso V, Vermelho AB, Santos-Oliveira R, Viçosa AL, Holandino C, Ricci-Júnior E, Development, characterization, and

anti-leishmanial activity of topical amphotericin B nanoemulsions, Drug Deliv. Transl. Res 10 (2020) 1552–1570, 10.1007/s13346-020-00821-5. [PubMed: 32676952]

[11]. Schuenck-Rodrigues RA, de Oliveira de Siqueira LB, dos Santos Matos AP, da Costa SP, da Silva Cardoso V, Vermelho AB, Colombo APV, Oliveira CA, Santos-Oliveira R, Ricci-Júnior E, Development, characterization and photobiological activity of nanoemulsion containing zinc phthalocyanine for oral infections treatment, J. Photochem. Photobiol. B, Biol 211 (2020), 112010, 10.1016/j.jphotobiol.2020.112010.

[12]. Singh JA, Saag KG, Bridges SL, Akl EA, Bannuru RR, Sullivan MC, Vaysbrot E, McNaughton C, Osani M, Shmerling RH, Curtis JR, Furst DE, Parks D, Kavanaugh A, O'Dell J, King C, Leong A, Matteson EL, Schousboe JT, Drevlow B, Ginsberg S, Grober J, St Clair EW, Tindall E, Miller AS, McAlindon T, American college of rheumatology guideline for the treatment of rheumatoid arthritis, Arthritis Rheumatol. 68 (2016) (2015) 1–26, 10.1002/art.39480. [PubMed: 26545940]

[13]. Smolen JS, Landewé RBM, Bijlsma JWJ, Burmester GR, Dougados M, Kerschbaumer A, McInnes IB, Sepriano A, Van Vollenhoven RF, De Wit M, Aletaha D, Aringer M, Askling J, Balsa A, Boers M, Den Broeder AA, Buch MH, Buttgereit F, Caporali R, Cardiel MH, De Cock D, Codreanu C, Cutolo M, Edwards CJ, Van Eijk-Hustings Y, Emery P, Finckh A, Gossec L, Gottenberg JE, Hetland ML, Huizinga TWJ, Koloumas M, Li Z, Mariette X, Müller-Ladner U, Mysler EF, Da Silva JAP, Poór G, Pope JE, Rubbert-Roth A, Ruyssen-Witrand A, Saag KG, Strangfeld A, Takeuchi T, Voshaar M, Westhovens R, Van Der Heijde D, EULAR recommendations for the management of rheumatoid arthritis with synthetic and biological disease-modifying antirheumatic drugs: 2019 update, Ann. Rheum. Dis 79 (2020) S685–S699, 10.1136/annrheumdis-2019-216655.

[14]. Carmichael SJ, Beal J, Day RO, Tett SE, Combination therapy with methotrexate and hydroxychloroquine for rheumatoid arthritis increases exposure to methotrexate, J. Rheumatol 29 (2002) 2077–2083 (Accessed June 9, 2021), https://pubmed.ncbi.nlm.nih.gov/12375315/. [PubMed: 12375315]

[15]. Yao Q, Choi JH, Dai Z, Wang J, Kim D, Tang X, Zhu L, Improving tumor specificity and anticancer activity of dasatinib by dual-targeted polymeric micelles, ACS Appl. Mater. Interfaces 9 (2017) 36642–36654, 10.1021/acsami.7b12233. [PubMed: 28960955]

[16]. Yao Q, Liu Y, Kou L, Tu Y, Tang X, Zhu L, Tumor-targeted drug delivery and sensitization by MMP2-responsive polymeric micelles, Nanomed. Nanotechnol., Biol. Med 19 (2019) 71–80, 10.1016/j.nano.2019.03.012.

[17]. Rollett A, Reiter T, Nogueira P, Cardinale M, Loureiro A, Gomes A, Cavaco-Paulo A, Moreira A, Carmo AM, Guebitz GM, Folic acid-functionalized human serum albumin nanocapsules for targeted drug delivery to chronically activated macrophages, Int. J. Pharm 427 (2012) 460–466, 10.1016/j.ijpharm.2012.02.028. [PubMed: 22374516]

[18]. Zhang Y, Song W, Geng J, Chitgupi U, Unsal H, Federizon J, Rzayev J, Sukumaran DK, Alexandridis P, Lovell JF, Therapeutic surfactant-stripped frozen micelles, Nat. Commun 7 (2016) 1–9, 10.1038/ncomms11649.

[19]. Zhang J, Fang X, Li Z, Chan HF, Lin ZX, Wang Y, Chen M, Redox-sensitive micelles composed of disulfide-linked pluronic-linoleic acid for enhanced anticancer efficiency of brusatol, Int. J. Nanomedicine 13 (2018) 939–956, 10.2147/IJN.S130696. [PubMed: 29491708]

[20]. Chen LC, Chen YC, Su CY, Wong WP, Sheu MT, Ho HO, Development and characterization of lecithin-based self-assembling mixed polymeric micellar (saMPMs) drug delivery systems for curcumin, Sci. Rep 6 (2016) 1–11, 10.1038/srep37122. [PubMed: 28442746]

[21]. Ahmad Z, Shah A, Siddiq M, Kraatz HB, Polymeric micelles as drug delivery vehicles, RSC Adv. 4 (2014) 17028–17038, 10.1039/c3ra47370h.

[22]. Tawfik SM, Azizov S, Elmasry MR, Sharipov M, Lee YI, Recent advances in nanomicelles delivery systems, Nanomaterials 11 (2021) 1–36, 10.3390/nano11010070.

[23]. Basak R, Bandyopadhyay R, Encapsulation of hydrophobic drugs in pluronic F127 micelles: effects of drug hydrophobicity, solution temperature, and pH, Langmuir. 29 (2013) 4350–4356, 10.1021/la304836e. [PubMed: 23472840]

[24]. Carvalho VFM, Salata GC, de Matos JKR, Costa-Fernandez S, Chorilli M, Steiner AA, de Araujo GLB, Silveira ER, Costa-Lotufo LV, Lopes LB, Optimization of composition and

obtainment parameters of biocompatible nanoemulsions intended for intraductal administration of piplartine (piperlongumine) and mammary tissue targeting, Int. J. Pharm 567 (2019), 10.1016/j.ijpharm.2019.118460.

[25]. Raval A, Pillai SA, Bahadur A, Bahadur P, Systematic characterization of Pluronic® micelles and their application for solubilization and in vitro release of some hydrophobic anticancer drugs, J. Mol. Liq 230 (2017) 473–481, 10.1016/j.molliq.2017.01.065.

[26]. ying Meng X, jia Li J, junhong Ni T, Xiao-tong L, He T, ning Men Z, sheng Liu J, Shen T, Electro-responsive brain-targeting mixed micelles based on Pluronic F127 and D-α-tocopherol polyethylene glycol succinate–ferrocene, Colloids Surfaces A Physicochem. Eng. Asp 601 (2020), 124986, 10.1016/j.colsurfa.2020.124986.

[27]. Jaiswal M, Dudhe R, Sharma PK, Nanoemulsion: an advanced mode of drug delivery system, 3 Biotech 5 (2015) 123–127, 10.1007/s13205-014-0214-0.

[28]. Masoumi HRF, Basri M, Samiun WS, Izadiyan Z, Lim CJ, Enhancement of encapsulation efficiency of nanoemulsion-containing aripiprazole for the treatment of schizophrenia using mixture experimental design, Int. J. Nanomed 10 (2015) 6469–6471, 10.2147/IJN.S89364.

[29]. Arbain NH, Basri M, Salim N, Wui WT, Abdul Rahman MB, Development and characterization of aerosol nanoemulsion system encapsulating low water soluble quercetin for lung cancer treatment, Mater. Today Proc (2018) S137–S142, 10.1016/j.matpr.2018.08.055. Elsevier Ltd.

[30]. Feng Z, Wang Z, Yang Y, Du Y, Cui S, Zhang Y, Tong Y, Song Z, Zeng H, Zou Q, Peng L, Sun H, Development of a safety and efficacy nanoemulsion delivery system encapsulated gambogic acid for acute myeloid leukemia in vitro and in vivo, Eur. J. Pharm. Sci 125 (2018) 172–180, 10.1016/j.ejps.2018.10.001. [PubMed: 30296572]

[31]. Chand Gupta Jyotshna A, Bawankule DU, Verma AK, Shanker K, Nanoemulsion preconcentrate of a pentacyclic triterpene for improved oral efficacy: Formulation design and in-vivo antimalarial activity, J. Drug Deliv. Sci. Technol 57 (2020), 101734, 10.1016/j.jddst.2020.101734.

[32]. Danaei M, Dehghankhold M, Ataei S, Hasanzadeh Davarani F, Javanmard R, Dokhani A, Khorasani S, Mozafari MR, Impact of particle size and polydispersity index on the clinical applications of lipidic nanocarrier systems, Pharmaceutics. 10 (2018), 10.3390/pharmaceutics10020057.

[33]. Jiang X, Bai C, Liu M, Nanotechnology for microfluidics, wiley (2019), 10.1002/9783527818341.

[34]. Fröhlich E, The role of surface charge in cellular uptake and cytotoxicity of medical nanoparticles, Int. J. Nanomed 7 (2012) 5577–5591, 10.2147/IJN.S36111.

[35]. Trivedi R, Kompella UB, Nanomicellar formulations for sustained drug delivery: strategies and underlying principles, Nanomedicine 5 (2010) 485–505, 10.2217/nnm.10.10. [PubMed: 20394539]

[36]. Gorain B, Choudhury H, Patro Sisinthy S, Kesharwani P, Polymeric micellebased drug delivery systems for tuberculosis treatment, Nanotechnol. Based Approaches Tuberc. Treat (2020) 175–191, 10.1016/b978-0-12-819811-7.00011-4. Elsevier.

[37]. Patel M, Kaneko T, Matsumura K, Switchable release nano-reservoirs for codelivery of drugs via a facile micelle-hydrogel composite, J. Mater. Chem. B 5 (2017) 3488–3497, 10.1039/c7tb00701a. [PubMed: 32264285]

[38]. Wang G, Wang JJ, Li F, To SST, Development and evaluation of a novel drug delivery: Pluronics/SDS mixed micelle loaded with myricetin in vitro and in vivo, J. Pharm. Sci 105 (2016) 1535–1543, 10.1016/j.xphs.2016.01.016. [PubMed: 26947760]

[39]. Kulthe SS, Inamdar NN, Choudhari YM, Shirolikar SM, Borde LC, Mourya VK, Mixed micelle formation with hydrophobic and hydrophilic pluronic block copolymers: Implications for controlled and targeted drug delivery, Colloids Surf. B Biointerfaces 88 (2011) 691–696, 10.1016/j.colsurfb.2011.08.002. [PubMed: 21862296]

[40]. Corrigan OI, Li X, Quantifying drug release from PLGA nanoparticulates, Eur. J. Pharm. Sci 37 (2009) 477–485, 10.1016/j.ejps.2009.04.004. [PubMed: 19379812]

[41]. Rajitha P, Biswas R, Sabitha M, Jayakumar R, Methotrexate in the treatment of psoriasis and rheumatoid arthritis: mechanistic insights, current issues and novel delivery approaches, Curr. Pharm. Des 23 (2017), 10.2174/1381612823666170601105439.

[42]. Friedman B, Cronstein B, Methotrexate mechanism in treatment of rheumatoid arthritis, Jt. Bone Spine 86 (2019) 301–307, 10.1016/j.jbspin.2018.07.004.

[43]. Van Ede AE, Laan RFJM, Rood MJ, Huizinga TWJ, Van De Laar MAFJ, Van Denderen CJ, Westgeest TAA, Romme TC, De Rooij DJRAM, Jacobs MJM, De Boo TM, Van Der Wilt GJ, Severens JL, Hartman M, Krabbe PFM, Dijkmans BAC, Breedveld FC, Van De Putte LBA, Effect of folic or folinic acid supplementation on the toxicity and efficacy of methotrexate in rheumatoid arthritis: A forty-eight-week, multicenter, randomized, double-blind, placebo-controlled study, Arthritis Rheum. 44 (2001) 1515–1524, 10.1002/1529-0131(200107)44:7<1515::AID-ART273>3.0.CO;2-7. [PubMed: 11465701]

[44]. Aletaha D, Smolen JS, Diagnosis and management of rheumatoid arthritis: a review, JAMA. 320 (2018) 1360–1372, 10.1001/jama.2018.13103. [PubMed: 30285183]

[45]. Wang W, Zhou H, Liu L, Side effects of methotrexate therapy for rheumatoid arthritis: A systematic review, Eur. J. Med. Chem 158 (2018) 502–516, 10.1016/j.ejmech.2018.09.027. [PubMed: 30243154]

[46]. Schrezenmeier E, Dörner T, Mechanisms of action of hydroxychloroquine and chloroquine: implications for rheumatology, Nat. Rev. Rheumatol 16 (2020) 155–166, 10.1038/s41584-020-0372-x. [PubMed: 32034323]

[47]. Schapink L, Van Den Ende CHM, Gevers LAHA, Van Ede AE, Den Broeder AA, The effects of methotrexate and hydroxychloroquine combination therapy vs methotrexate monotherapy in early rheumatoid arthritis patients, Rheumatol. (United Kingdom) 58 (2019) 131–134, 10.1093/rheumatology/key275.

[48]. Micsik T, Lorincz A, Gál J, Schwab R, Peták I, MDR-1 and MRP-1 activity in peripheral blood leukocytes of rheumatoid arthritis patients, Diagn. Pathol 10 (2015), 10.1186/s13000-015-0447-1.

[49]. Hider SL, Owen A, Hartkoorn R, Khoo S, Back D, Silman AJ, Bruce IN, Down regulation of multidrug resistance protein-1 expression in patients with early rheumatoid arthritis exposed to methotrexate as a first disease-modifying antirheumatic drug, Ann. Rheum. Dis 65 (2006) 1390–1393, 10.1136/ard.2005.049189. [PubMed: 16504991]

[50]. Caparroz-Assef SM, Bersani-Amado CA, Kelmer-Bracht AM, Bracht A, Ishii-Iwamoto EL, The metabolic changes caused by dexamethasone in the adjuvant-induced arthritic rat, Mol. Cell. Biochem 302 (2007) 87–98, 10.1007/s11010-007-9430-9. [PubMed: 17347874]

[51]. Mahmoud AM, Hozayen WG, Ramadan SM, Berberine ameliorates methotrexate-induced liver injury by activating Nrf2/HO-1 pathway and PPARγ, and suppressing oxidative stress and apoptosis in rats, Biomed. Pharmacother 94 (2017) 280–291, 10.1016/j.biopha.2017.07.101. [PubMed: 28763751]

[52]. Brackertz D, Mitchell GF, Mackay IR, Antigen-induced arthritis in mice, Arthritis Rheum. 20 (1977) 841–850, 10.1002/art.1780200314. [PubMed: 857805]

[53]. Beringer A, Miossec P, Systemic effects of IL-17 in inflammatory arthritis, Nat. Rev. Rheumatol 15 (2019) 491–501, 10.1038/s41584-019-0243-5. [PubMed: 31227819]

[54]. Yu R, Li X, DuBois DC, Almon RR, Cao Y, Jusko WJ, Interactions of tofacitinib and dexamethasone on lymphocyte proliferation, Pharm. Res 37 (2020), 10.1007/s11095-020-02827-7.

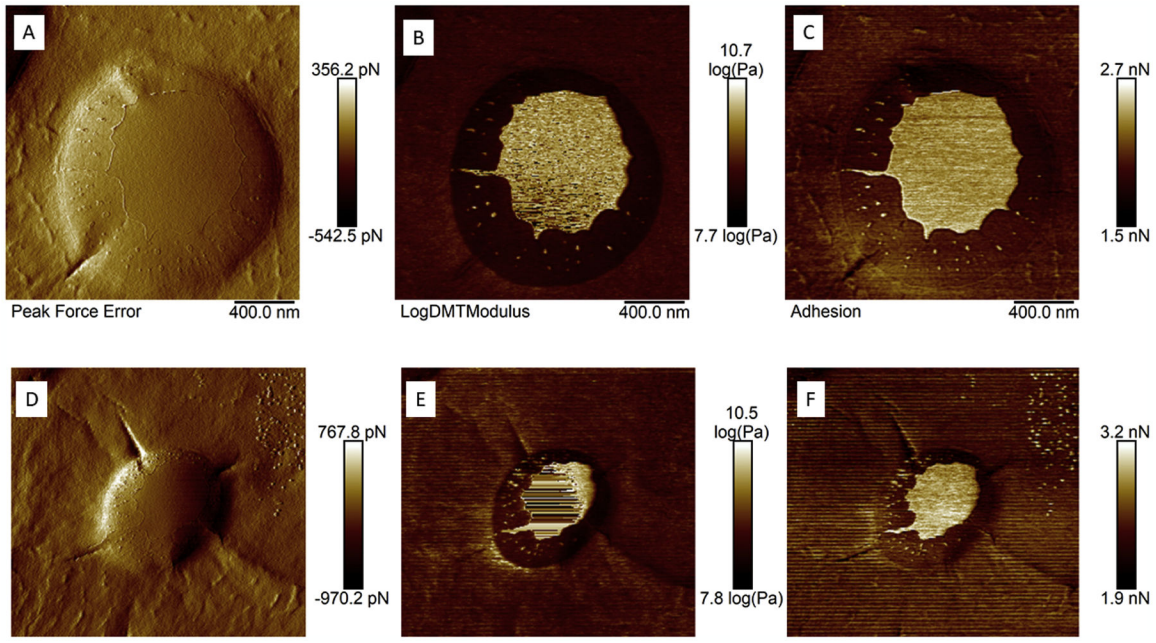

Fig. 1.

Topography images (Peak Force Error – Figures A and D), Young's modulus maps (Figures B and E) and adhesion force maps (Figures C and F) of individual 127–Pluronic–HCQ-MTX-nanomicelles.

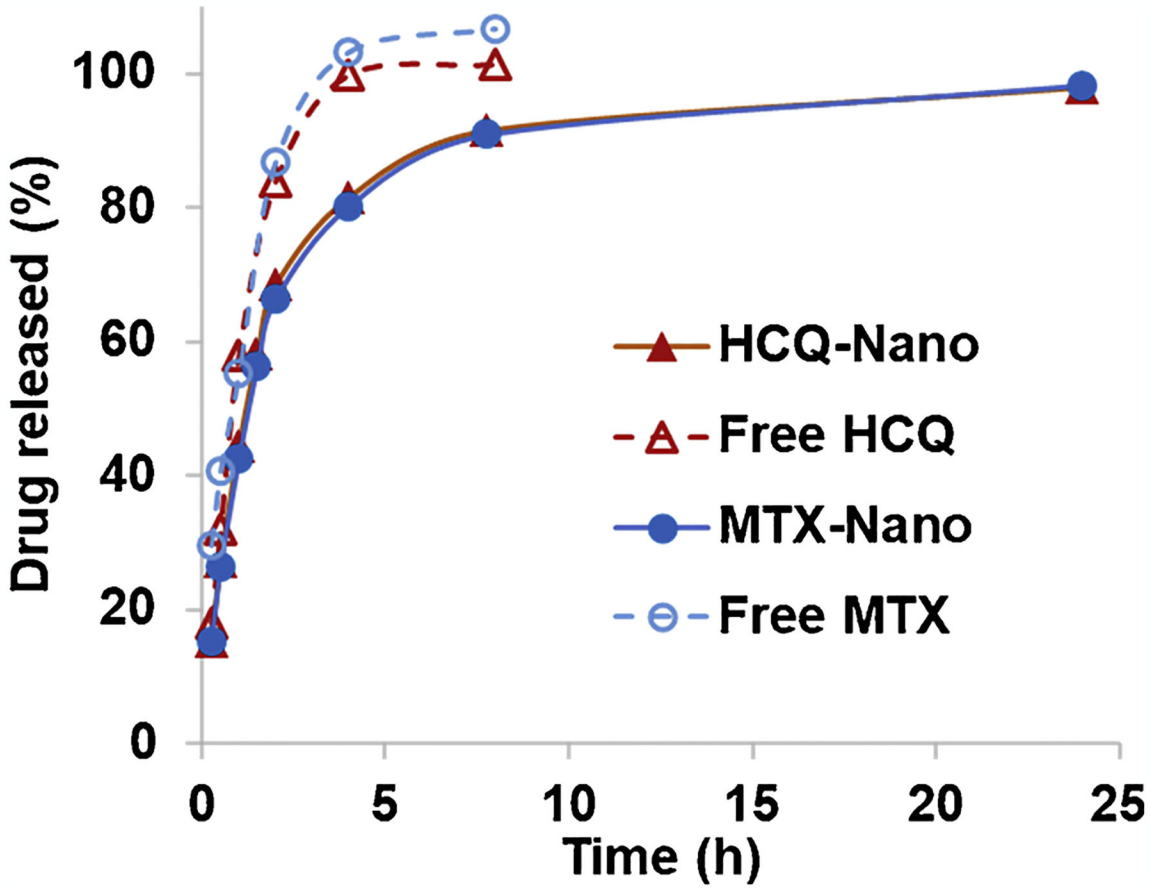

Fig. 2.

In vitro accumulative drug release from the Pluronic–HCQ-MTX-nanomicelles. The samples were dialyzed (MWCO 12,000–14,000 Da) against PBS containing 0.1 % Tween 80 at 37 °C, to simulate the “sink condition”.

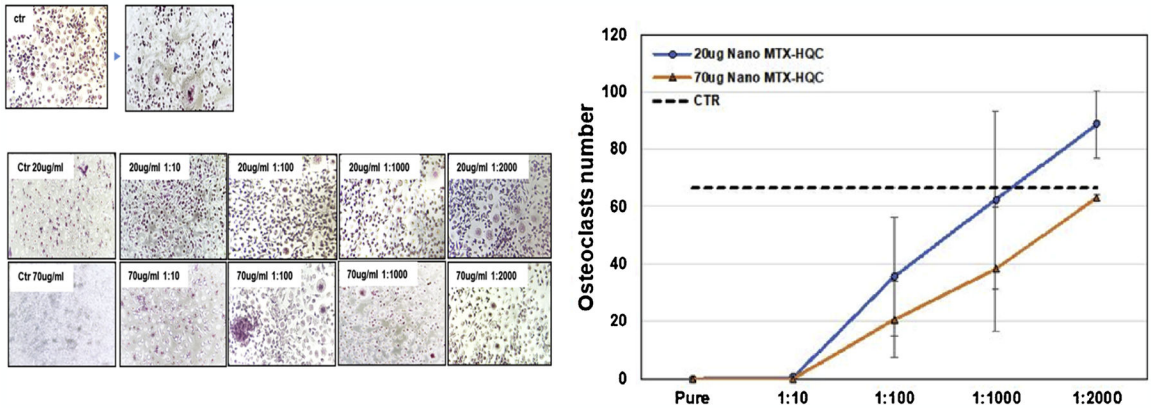

Fig. 3.

Evaluation of osteoclastogenesis after in vitro treatment with HCQ + MTX-loaded nanomicelles in two concentrations: 20 ug/mL HCQ +0.74 ng/mL MTX and 70 ug/mL HCQ +2.6 ng/mL MTX), in different dilutions. **3B:** Representative graph of the number of osteoclasts after in vitro treatment with HCQ + MTX-loaded nanomicelles in two concentrations: 20 ug/mL HCQ +0.74 ng/mL MTX and 70 ug/mL HCQ +2.6 ng/mL MTX), in different dilutions.

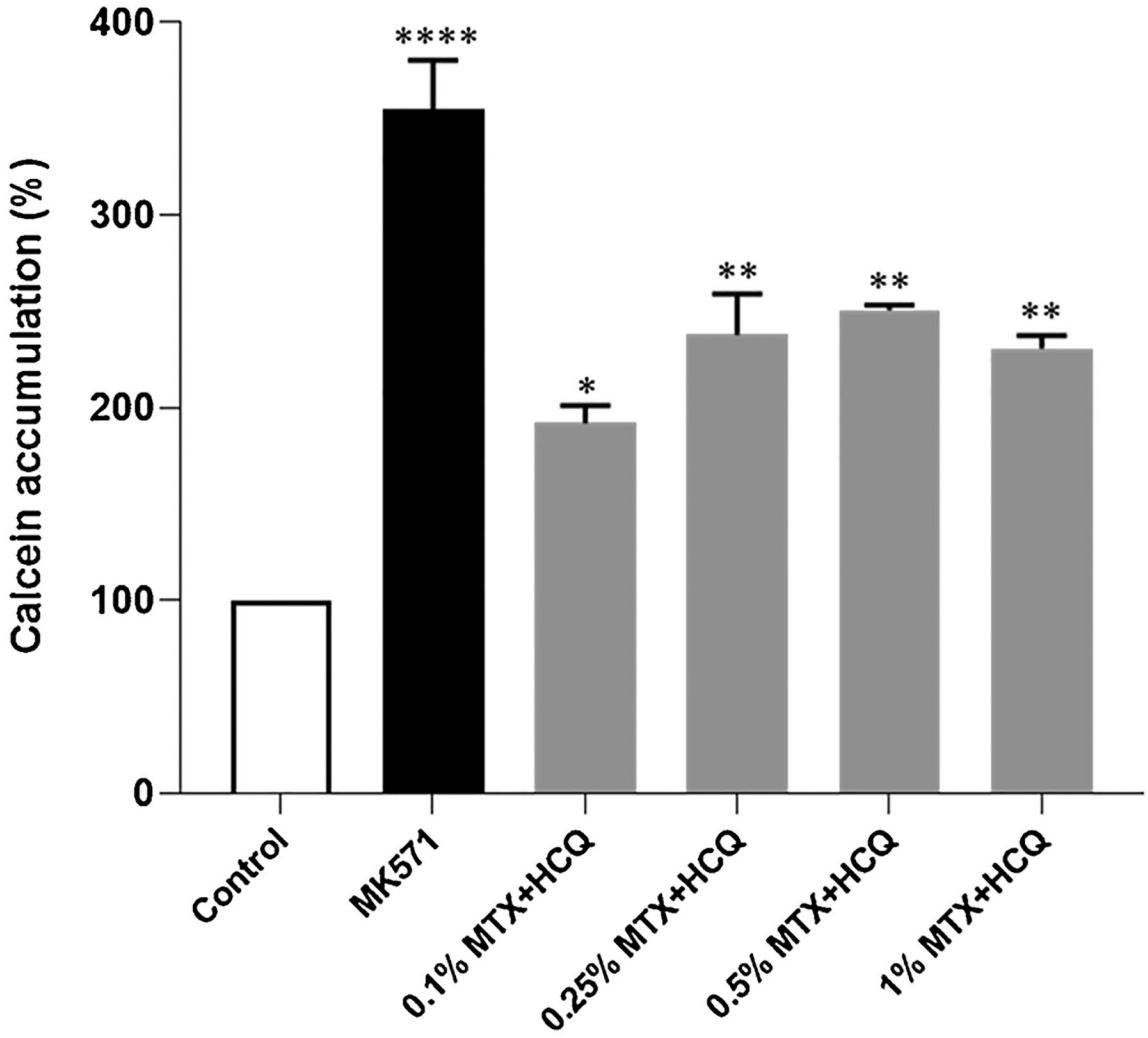

Fig. 4.

Effect of 127-Pluronic–HCQ-MTX Nanomicelle on MRP1 mediated efflux activity. HEK293/MRP1 cells were treated with various concentration (0.1 %, 0.25 %, 0.5 % and 1% all % w/v) of the test compound, and 50μM of MK571 (positive control) for 10 min at 37 °C before treatment with 0.25 μM calcein-AM for 30 min. Flow cytometric measurements of intracellular calcein-AM was conducted at 488 nm and 533/30 nm for excitation and emission wavelengths, respectively. Experiments were done as triplicates in two independent experiments and presented as mean ± S.E.M. *P < 0.05; **P < 0.01; ***P < 0.001 compared to control.

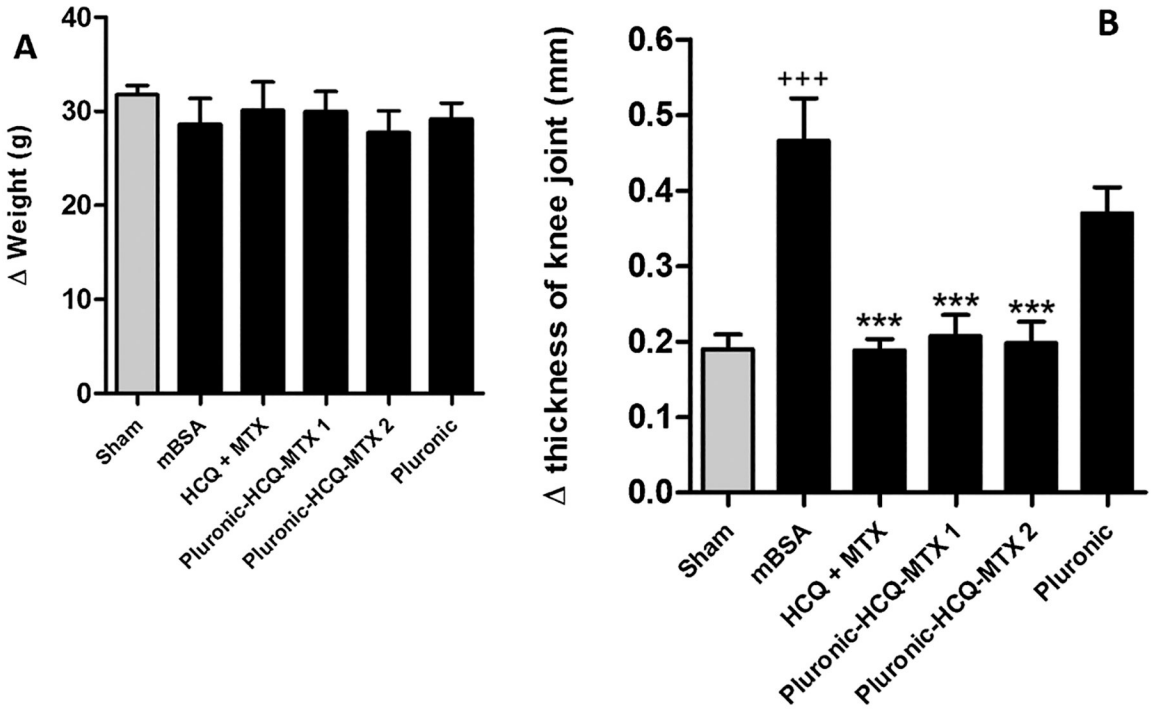

Fig. 5.

A: Body weight assessment. Twenty-one days after antigen induction of RA, the animals were treated daily with HCQ + MTX, 127-Pluronic–HCQ-MTX nanomicelles 1 or 127-Pluronic–HCQ-MTX nanomicelles 2 via i.p. for seven days. The animals in the control group (sham) and in the immunized group (mBSA) were administered intraperitoneally with sterile saline. The animals in the vehicle group were administered intraperitoneally with Pluronic 10 %. The results are presented as the mean of the differences between pre-treatment and post-treatment weight (Δ) ± SEM of five mice per group. **5B**:**127-Pluronic–HCQ-MTX nanomicelles reduces antigen-induced edema.** Knee joint edema was assessed by measuring the transverse diameter of thefemur-tibial joint with the aid of a digital caliper (Digmatic caliper, Mitutoyo Corp. Kanagawa, Japan). The edema values were expressed by the difference (Δ) between the diameters measured before (baseline) and after ± SEM treatment and were represented in millimeters (mm). +++ $p < 0.001$ compared to sham group; *** $p < 0.001$ compared to mBSA group.

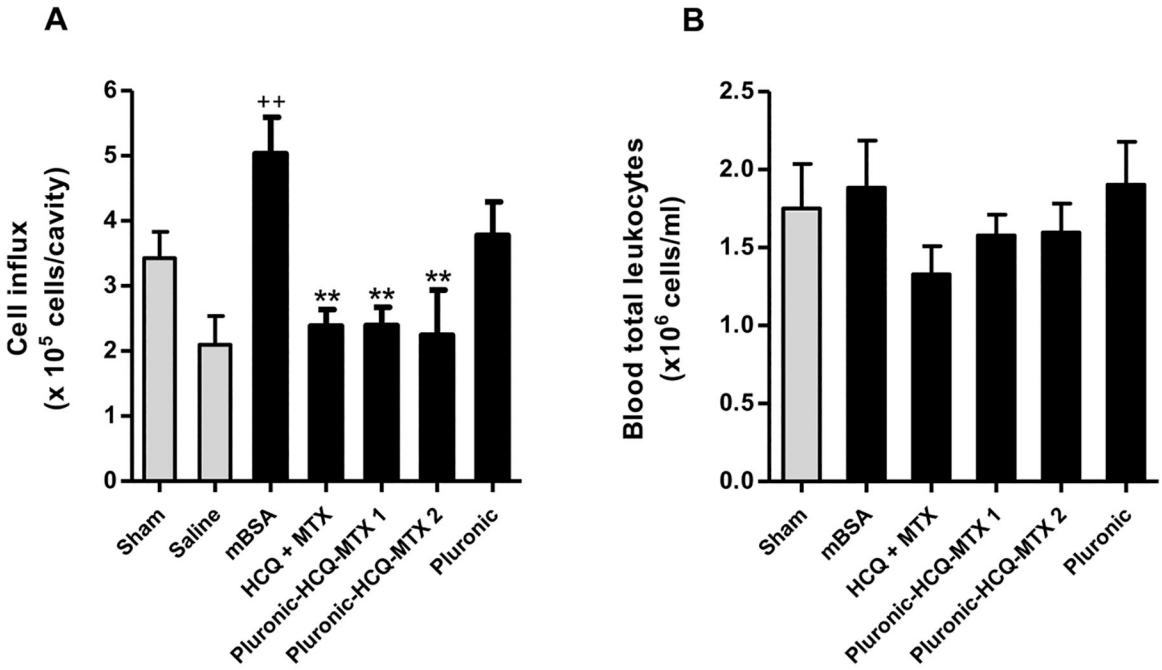

Fig. 6.

127-Pluronic–HCQ-MTX nanomicelles inhibits inflow of cells into the joint cavity. (A) The number of leukocytes present in the femurtibial joint was assessed by counting the total number of leukocytes present in the synovial lavage and the analysis performed using an automatic microparticle counter (Z1; Beckman-Coulter, USA). The results were presented as number of cells $x10^5 \pm$ SEM. + + $p < 0.01$ compared to saline group. ** $P < 0.01$ compared to mBSA group. (B) The number of total circulating leukocytes was evaluated in the blood supernatant after centrifugation and the analysis was carried out using the automatic microparticle counter. The results were presented as number of cells $x10^6 \pm$ SEM.

Table 1

Treatments administered to different groups after induction of experimental arthritis.

Group	Treatment
Sham	Sterile saline
Saline	Sterile saline
mBSA	Sterile saline
Pluronic	Pluronic 10 % (pure solution)
HCQ + MTX	HCQ: 2 mg/kg + MTX: 1 mg/kg
127-Pluronic-HCQ-MTX nanomicelles 1	HCQ: 2 mg/kg + MTX: 1 mg/kg
127-Pluronic-HCQ-MTX nanomicelles 2	HCQ: 1 mg/kg + MTX: 0,5 mg/kg

Table 2

Values referring to the average size by dynamic light scattering and zeta potential of the nanomicelles loaded with HCQ plus MTX.

Parameter	Value
Hydrodynamic diameter	48,323 nm (SD 4842 nm)
PDI	0256 (SD 196)
Zeta potential	059 mV (SD 008 mV)
Conductivity	391 mS/cm (SD 009 mS/cm)
Electrophoretic mobility	005 μm.cm/Vs (SD 001 μm.cm/Vs)